Robust Subnanometric Plasmon Ruler by Rescaling of the Nonlocal Optical Response

T. V. Teperik,[1] P. Nordlander,[2] J. Aizpurua,[3] and A. G. Borisov[4]

[1]*Institut d'Electronique Fondamentale, UMR 8622 CNRS-Université Paris-Sud, Bâtiment 220, 91405 Orsay Cedex, France*
[2]*Department of Physics and Astronomy, M.S. 61 Laboratory for Nanophotonics, Rice University, Houston, Texas 77251-1892, USA*
[3]*Material Physics Center, CSIC-UPV/EHU and Donostia International Physics Center DIPC, Paseo Manuel de Lardizabal 5 20018, Donostia-San Sebastián, Spain*
[4]*Institut des Sciences Moléculaires d'Orsay, UMR 8214 CNRS-Université Paris-Sud, Bâtiment 351, 91405 Orsay Cedex, France*

(Received 18 March 2013; published 28 June 2013)

We present the optical response of two interacting metallic nanowires calculated for separation distances down to angstrom range. State-of-the-art local and nonlocal approaches are compared with full quantum time-dependent density functional theory calculations that give an exact account of nonlocal and tunneling effects. We find that the quantum results are equivalent to those from classical approaches when the nanoparticle separation is defined as the separation between centroids of the screening charges. This establishes a universal plasmon ruler for subnanometric distances. Such a ruler not only impacts the basis of many applications of plasmonics, but also provides a robust rule for subnanometric metrology.

DOI: 10.1103/PhysRevLett.110.263901 PACS numbers: 42.25.Bs, 36.40.Gk, 73.20.Mf, 78.67.Bf

The exact calculation of the optical response of a nanosystems is a challenging task. In metallic nanostructures the complex nonlocal interactions between conduction electrons modify the standard local classical response, typically characterized by the presence of surface plasmon resonances [1]. This effect is more pronounced in small particles and in strongly coupled systems where the nonlocal nature of electronic interactions is emphasized. To establish an exact and accurate model to describe the spectral features of plasmonic resonances in such systems is thus of paramount importance from both fundamental and practical points of view [2,3]. A variety of theoretical approaches that incorporate different levels of sophistication have been adopted to address the optical response, but certain lack of unification still persists. In particular, the community of surface physics has elaborated accurate nonlocal treatments to address the surface response of conduction electrons of metal surfaces and small metallic objects [1,4–9], whereas the community of nano-optics has focused on developing practical local and nonlocal treatments where the emphasis is placed on the geometrical aspects of the metal boundaries rather than on the actual response of the electrons [2,3,10–16]. This Letter bridges both fields, providing a unified and practical picture of the optical response in coupled metallic nanoparticles located at subnanometric proximity.

We calculate the optical response of two interacting metallic nanowires in vacuum using a full quantum time-dependent density functional theory (TDDFT) approach [17] as well as using macroscopic theory based on solution of classical Maxwell equations with local and nonlocal descriptions of the system. The comparison between quantum and classical results on coupled nanowires provides a perfect basis to unravel the limitations, tendencies, and physics of the optical response under different levels of approximation. By doing so, we are able to relate the results of the optical response from different approximations and predict the influence of nonlocality in the limit of subnanometric distances where nonlocal effects are pronounced. In elucidating the major physics behind the nonlocal response in plasmonic nanoparticle dimer, we find a robust plasmon ruler [18–22] that unambiguously determines the spectral position of surface plasmon resonances in strongly coupled systems forming subnanometric plasmonic cavities.

To implement the TDDFT calculations, a cylindrical jellium model is adopted to describe the electronic structure of the infinite metallic nanowire. This model captures the collective plasmonic modes of conduction electrons and is perfectly suited to address nonlocal effects derived from the interactions between these electrons, such as the dynamical screening of the external field [1,4,5] and tunneling [23–27] as discussed below. Within the jellium model, the ionic cores of the nanowire atoms are represented with a uniform background charge density $n_0 = 3/4\pi r_s^3$. The screening radius r_s is set equal to $4a_0$ (Bohr radius $a_0 = 0.053$ nm) corresponding to sodium which is a prototypical free-electron metal. We have performed the calculations for $D = 6.2$ nm and $D = 9.8$ nm diameter nanowires, where the circle of diameter D provides the position of the jellium edge separating uniform positive background from the vacuum. The jellium edge is located at half a lattice constant ($a = 4.23$ Å for Na) in front of the plane of surface atoms. The optical response of the isolated nanowire and nanowire dimer has been obtained within the Kohn-Sham scheme of TDDFT [17] as detailed in Ref. [25].

Along with the TDDFT study, we have performed classical Maxwell calculations of the optical extinction. Different levels of sophistication have been adopted using (i) the local Drude description of sodium permittivity

$\varepsilon(\omega) = 1 - \omega_p^2/\omega(\omega + i\gamma)$, where $\omega_p = 5.89$ eV is the bulk plasma frequency of Na and γ accounts for the damping, (ii) the nonlocal hydrodynamic model (NLHD) [10,13–16] description of the metal permittivity tensor as implemented by Toscano and co-workers in the COMSOL MULTIPHYSICS package [15,28], and (iii) the quantum-corrected model (QCM) [29] allowing us to perform classical calculations that take into account electron tunneling through the junction separating nanowires. The particular application of QCM for a sodium dimer is described in detail in Ref. [23]. Finally, in all classical models above we used $\gamma = 0.16$ eV, which provides the best match with the TDDFT results.

Prior to the discussion of the spectral plasmon peaks for nanowire dimer, we consider an isolated nanowire. This allows us to distinguish between the effects that are inherent to an individual nanoparticle and those which are associated with the Coulomb coupling between the wires. In Fig. 1(a) we show the extinction cross section of the isolated nanowire [30]. The TDDFT result displays a well-formed dipolar plasmon resonance at frequency $\omega_{sp} = 4.072$ eV redshifted from the classical Drude value $\omega_{sp}^D = \omega_p/\sqrt{2} = 4.14$ eV. This shift of the plasmon resonance is a nonlocal finite size effect linked with the dynamical screening of the fields by conduction electrons. As has been thoroughly studied in the context of metal clusters [8,9,31–33],

$$\omega_{sp}/\omega_{sp}^D = 1 - \mathrm{Re}[d(\omega_{sp}^D)]/R_{cl} + O(R_{cl}^{-2}), \qquad (1)$$

where R_{cl} is the cluster radius and $\mathrm{Re}[d(\omega_{sp})]$ is the real part of the Feibelman parameter that gives the position of the centroid of the induced surface charge density with respect to the jellium edge [4–6]. As follows from quantum calculations for free-electron metals, because of the spill out of conduction electrons, the screening charge resides outside metal surface. The $\mathrm{Re}[d(\omega_{sp})]$ is thus positive, which explains the redshift of the dipolar plasmon for alkali metals. From our results we obtain $\mathrm{Re}[d(\omega_{sp})] \sim 1$ Å, in agreement with earlier experimental and theoretical data [4,5,31–33].

In contrast to the TDDFT, in the NLHD treatment the dipole plasmon frequency appears blueshifted with respect to the ω_{sp}. The plasmon-induced charges in the NLHD are localized within a layer of thickness $\delta = \beta/\omega_p$ below the metal surface [14], where β is the hydrodynamic nonlocality parameter [28]. The effective $\mathrm{Re}[d(\omega)]$ is thus always negative leading to a blueshift of the localized plasmon irrespective of the metal. This is in contradiction with both quantum and experimental data for alkali clusters. For noble metals, because of the contribution to the screening of the localized d electrons, the centroid of the screening charge is inside the metal surface [5,9]. Thus, for Au and Ag nanoparticles the dipolar plasmon resonance experiences a blueshift [9,34–36]. The qualitative agreement of NLHD with full quantum treatments and experiments is, however, fortuitous in this case, because the NLHD description associates the effect with conduction electrons only.

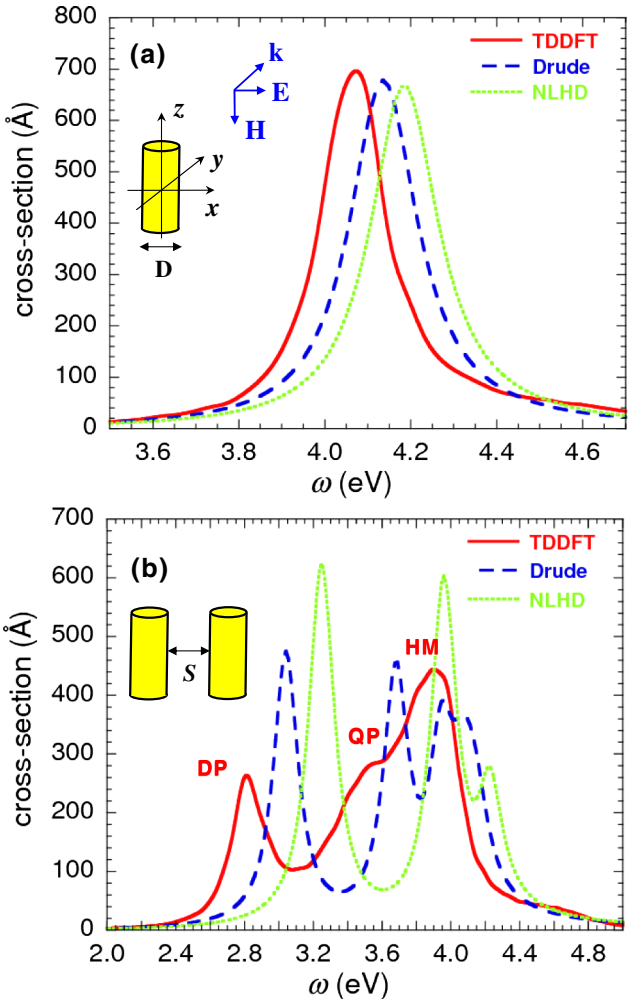

FIG. 1 (color online). Extinction cross section per length for (a) isolated jellium nanowire of diameter $D = 9.8$ nm. Results are shown as a function of the frequency ω of the incident radiation. The incoming field is an x-polarized plane wave as depicted in the inset. The results from TDDFT calculations are compared with those from classical electromagnetic calculations using local (Drude) and nonlocal hydrodynamic response (NLHD). (b) Same as in (a) but for a jellium nanowire dimer with junction size $S = 7.4$ Å.

Figure 1(b) shows the response of a pair of identical parallel nanowires of $D = 9.8$ nm diameter separated by the distance $S = 7$ Å, as measured between the jellium edges. The TDDFT result features the bonding dipole plasmon (DP) mode at 2.8 eV and quadrupolar mode (QP) at 3.5 eV. Because of the attractive interaction between the plasmon-induced screening charges of opposite sign at facing surfaces across the junction, these modes are shifted from the higher order hybridized mode (HM) at $\omega = 3.9$ eV close to ω_{sp}. For large separation S, the DP and QP modes merge into the HM and the spectrum evolves into that of the individual nanowire. Similar to an

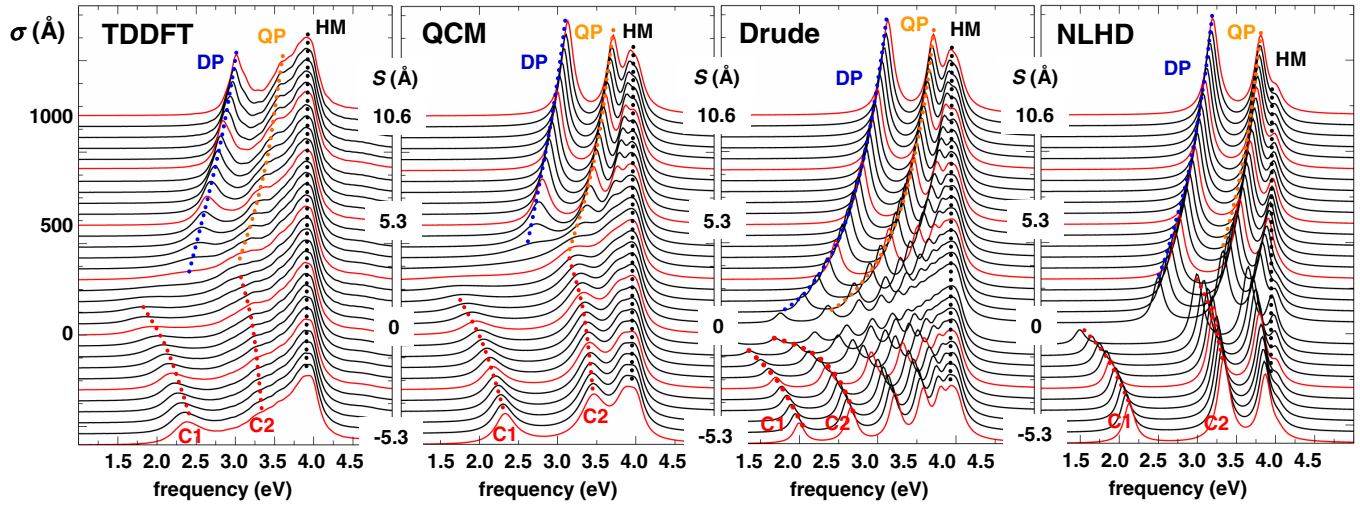

FIG. 2 (color online). Extinction cross section σ per length calculated with different approaches for the D ¼ 9.8 nm Na nanowire dimer in vacuum. The incoming plane wave is polarized along the dimer axis x. Waterfall plots show the results as a function of the frequency of the incoming radiation for different junction widths S varied in steps of $1a_0$ ¼ 0.53 Å. Red curves (gray) correspond to S ¼ □5.3, □2.65, 0, 2.65, 5.3, 7.95, and 10.6 Å. For further details, see the text.

individual nanowire, the resonances in TDDFT are redshifted with respect to the classical Drude results whereas the NLHD gives a blueshift of the resonances.

For the nanowire dimer, the dynamic screening affects the energies of plasmonic modes through the shift of the plasmon frequency of the isolated nanowire and through the change of the coupling across the junction. As we will show below, the latter effect is relevant for plasmon ruler applications. To unravel its role we have performed calculations of the optical response of the parallel nanowire dimer by varying the width of the junction S. The plasma frequency parameter ω_p in classical descriptions has been adjusted [37] to obtain an agreement with TDDFT at large separation S ¼ 25 Å, thus isolating the effects of coupling and removing the differences arising from the different descriptions of the isolated nanowire. Observe that, according to Eq. (1), large systems would not require correction.

In Fig. 2 we compare TDDFT, QCM, classical Drude, and NLHD results for different junction widths S. The negative S means a geometrical overlap of the nanowires. The S ¼ 0 case corresponds to kissing cylinders [13,14] where a continuous solid is formed at the contact point. For large positive separations classical models qualitatively agree with TDDFT results. The absorption spectrum is dominated by several resonant structures [13,14,38,39]: a DP and a QP partially mixed with higher order modes HM. As S decreases, the DP and QP shift to lower frequencies because of the attractive interaction between the charges of opposite sign across the junction [40]. For junction widths $S \lesssim 7$ Å, electron tunneling across the junction becomes large and we retrieve the main trends reported theoretically for nanodimers [23–25,41] and confirmed in recent pioneering experiments [26,27]. Prior to the direct contact: the field enhancement in the middle of the junction is quenched, the DP resonance progressively disappears, a charge transfer plasmon mode ($C1$) emerges, and the QP continuously evolves into a higher order charge transfer plasmon $C2$. For an overlapping dimer with well established conductive contact, the $C1$ and $C2$ experience a blueshift [42].

While equivalent to the classical Drude description for large S, the QCM accounts for the tunneling in narrow junctions and reproduces the quantum results. As for the classical Drude and NLHD descriptions, they do not account for tunneling and fail for $S \lesssim 7$ Å. Indeed, the accumulation of classical charges on the opposite sides of the junction leads to diverging local fields and a dense number of resonances [2,3,40,43]. With NLHD the divergence of the fields in the junction is removed [13,14]; however, as compared to TDDFT the fields are too large. The number of resonances remains small but larger than in TDDFT and QCM, and transition from separated to overlapping regime appears nonphysically abrupt.

For the junction widths $S > 7$ Å, the detailed analysis of the frequency of the DP calculated with different approaches is shown in Fig. 3(a) as function of S. The same trends as in Fig. 1(b) are observed. The DP frequency obtained with TDDFT (NLHD) is noticeably redshifted (blueshifted), with respect to classical Drude calculations. We recall here that applied frequency correction isolates the effects of coupling and removes the differences arising from the different descriptions of the isolated nanowire. Since in this distance range the tunneling can be neglected, the dependence of the DP frequency on S results from the interaction between the screening charges induced across the junction. Thus, the classical Drude model underestimates the interaction between the screening charges and this underestimate is even stronger for NLHD approach.

To understand the above result we explore the definition of the width of the junction based on the separation between

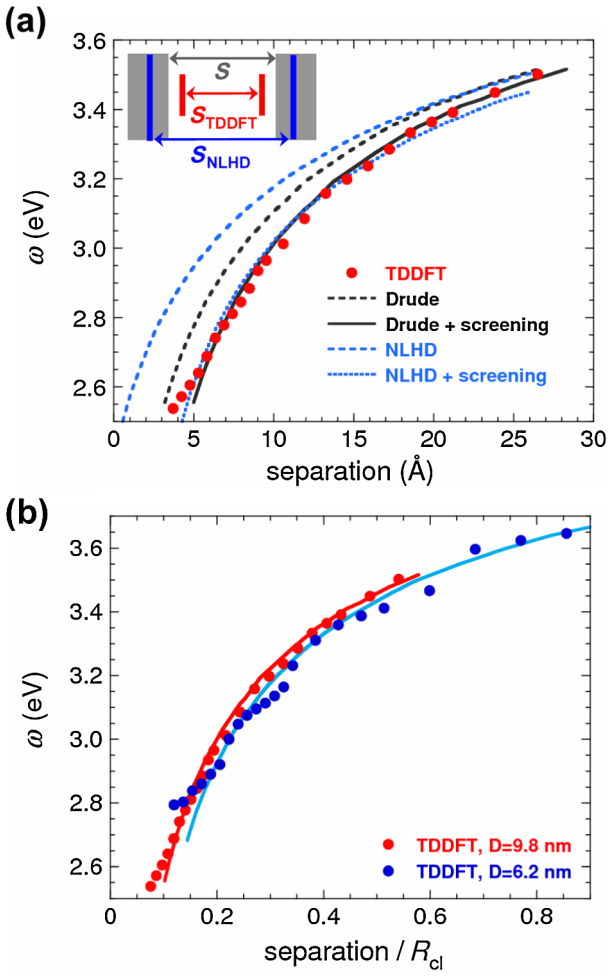

FIG. 3 (color online). (a) Energy of the dipole plasmon resonance as a function of the junction width S for a $D = 9.8$ nm nanowire dimer. Dots: TDDFT results; dashed and solid black lines: results of classical Drude calculations performed for the junction widths S and $S - 2\Delta$, respectively; dashed and dotted blue lines: results of NLHD calculations performed for the junction widths S and $S - 2\Delta - 2\delta$, respectively. The inset gives schematic representation of the location of plasmon-induced screening charges in various approaches. (b) Energy of the dipole plasmon resonance for $D = 6.2$ nm and $D = 9.8$ nm nanowire dimers as a function of the scaled separation S/R_{cl}. Solid lines: classical Drude calculations performed for the junction width $S - 2\Delta$.

the centroids of the screening charge at facing surfaces. We show that this measure of the junction size provides a universal, model independent dispersion of the DP frequency. The schematic representation underlying the discussion below is shown in the inset of Fig. 3(a). Within the local classical approach, the induced screening charges are localized at geometrical surfaces of the cylinders separated by the distance S. Within the TDDFT, the position of the induced charges with respect to the jellium edge is given by positive $\Delta = \mathrm{Re}[d(\omega)] - 0.9$ Å in the frequency range of interest [4,6,9]. The effective distance, $S_{TDDFT} = S - 2\Delta$, between the plasmon-induced charges across the junction is thus smaller than S measured between jellium edges. As discussed earlier, in the NLHD the screening charge is shifted inside the geometrical surface of the metal by $\delta \sim 1$ Å. Therefore, within the NLHD approach the screening charges are separated by a distance $S_{NLHD} = S + 2\delta$, which is larger than S. As follows from the results presented in Fig. 3(a), when the energy of the DP mode ω is taken at the same distance between the screening charges, the agreement between the results of TDDFT, Drude, and NLHD simulations becomes excellent: $\omega_{TDDFT}(S) \sim \omega_{Drude}(S - 2\Delta) \sim \omega_{NLHD}(S - 2\Delta - 2\delta)$. Thus, for not too narrow junctions where tunneling is negligible, the full quantum results can be retrieved within local classical calculations performed for the junction width given by the actual separation between the screening charges. At this point it is worth stressing that $\mathrm{Re}[d(\omega)]$ is a material and frequency dependent function, but it is independent of the geometry as follows from calculations and experiments performed for the clusters of different size and for flat surfaces [4,5,8,9,31–33].

The results above have direct implications for the ultimate limit of resolution of plasmonic rulers [22]. For the free-electron Na surface, the screening charges are located at approximately 0.9 Å (3 Å) outside the jellium edge (surface atomic layer), meaning that for a Na-Na junction, the effective junction width obtained from matching the measured DP frequency with local classical Drude calculations would be 1.8 Å (6 Å) smaller than the actual separation between the jellium edges (surface atomic planes). For silver and gold, an analysis of the data on the blueshift of the dipole plasmon resonance in small clusters [9,27,34,44] using Eq. (1) places the effective screening charges inside the jellium edge at 0.8–1.5 Å. Therefore, for Ag-Ag and Au-Au junctions, the effective junction width obtained from matching an experiment to local classical calculations would be by 1.7–3 Å larger than the actual separation between the jellium edges. It will be close to the separation between the surface atomic planes.

The use of the plasmon ruler relies on the universal dependence of the DP frequency on the scaled separation [18,21]. In Fig. 3(b) we show the TDDFT and classical results for the DP frequency of the $D = 6.2$ nm and $D = 9.8$ nm nanowire dimers as a function of the scaled separation S/R_{cl}. The TDDFT data for both nanowire dimer sizes nearly fall on the universal curve provided that the separations S are sufficiently large that no tunneling occurs. This holds for junction widths larger than 2 lattice constants, which sets a lowest limit for the distances that can be actually measured with a plasmon ruler.

In conclusion, we have presented a fully quantum mechanical study of the optical response of a plasmonic nanowire dimer. The concept of rescaling of separation distances as introduced here allows for establishing a robust and novel rule of thumb to perform accurate

metrology of subnanometric distances based on the plasmonic dispersion. Our results are valid not only for the interaction of nanowires considered here, but can be extended to general junctions between metallic surfaces where nonlocal effects are extremely important.

We thank Guiseppe Toscano for providing the NPL extension to COMSOL 4. 2a RF Module used in our nonlocal calculations as well as for his kind assistance. J. A. acknowledges financial support from the ETORTEK project *nanoiker* of the Department of Industry of the Basque Government and Grant No. FIS2010-19609-C02-01 from the Spanish Ministry of Innovation. P. N. Acknowledges support from the Robert A. Welch Foundation (Grant No. C-1222) and the Office of Naval Research (Grant No. N00014-10-1-0989).

[1] J. M. Pitarke, V. M. Silkin, E. V. Chulkov, and P. M. Echenique, Rep. Prog. Phys. **70**, 1 (2007).
[2] J. A. Schuller, E. S. Barnard, W. Cai, Y. C. Jun, J. S. White, and M. L. Brongersma, Nat. Mater. **9**, 193 (2010).
[3] N. J. Halas, S. Lal, W.-S. Chang, S. Link, and P. Nordlander, Chem. Rev. **111**, 3913 (2011).
[4] P. J. Feibelman, Prog. Surf. Sci. **12**, 287 (1982).
[5] A. Liebsch, Phys. Rev. B **36**, 7378 (1987).
[6] P. Apell, Å. Ljungbert, and S. Lundqvist, Phys. Scr. **30**, 367 (1984).
[7] X. Wang and K. Kempa, Phys. Rev. B **75**, 245426 (2007).
[8] P. Apell and Å. Ljungbert, Solid State Commun. **44**, 1367 (1982).
[9] A. Liebsch, Phys. Rev. B **48**, 11 317 (1993).
[10] F. J. García de Abajo, J. Phys. Chem. C **112**, 17 983 (2008).
[11] J. M. McMahon, S. K. Gray, and G. C. Schatz, Phys. Rev. Lett. **103**, 097403 (2009).
[12] C. Ciracì, R. T. Hill, J. J. Mock, Y. Urzhumov, A. I. Fernández-Domínguez, S. A. Maier, J. B. Pendry, A. Chilkoti, and D. R. Smith, Science **337**, 1072 (2012).
[13] A. I. Fernández-Domínguez, A. Wiener, F. J. García-Vidal, S. A. Maier, and J. B. Pendry, Phys. Rev. Lett. **108**, 106802 (2012).
[14] A. I. Fernández-Domínguez, P. Zhang, Y. Luo, S. A. Maier, F. J. García-Vidal, and J. B. Pendry, Phys. Rev. B **86**, 241110(R) (2012).
[15] G. Toscano, S. Raza, A.-P. Jauho, N. A. Mortensen, and M. Wubs, Opt. Express **20**, 4176 (2012).
[16] G. Toscano, S. Raza, S. Xiao, M. Wubs, A.-P. Jauho, S. I. Bozhevolnyi, and N. A. Mortensen, Opt. Lett. **37**, 2538 (2012).
[17] M. A. L. Marques and E. K. U. Gross, Annu. Rev. Phys. Chem. **55**, 427 (2004).
[18] L. Gunnarsson, T. Rindzevicius, J. Prikulis, B. Kasemo, M. Käll, S. Zou, and G. C. Schatz, J. Phys. Chem. B **109**, 1079 (2005).
[19] N. Liu, M. Hentschel, T. Weiss, A. P. Alivisatos, and H. Giessen, Science **332**, 1407 (2011).
[20] S. S. Aćimović, M. P. Kreuzer, M. U. González, and R. Quidant, ACS Nano **3**, 1231 (2009).
[21] P. K. Jain, W. Huang, and M. A. El-Sayed, Nano Lett. **7**, 2080 (2007).
[22] R. T. Hill, J. J. Mock, A. Hucknall, S. D. Wolter, N. M. Jokerst, D. R. Smith, and A. Chilkoti, ACS Nano **6**, 9237 (2012).
[23] R. Esteban, A. G. Borisov, P. Nordlander, and J. Aizpurua, Nat. Commun. **3**, 825 (2012).
[24] J. Zuolaga, E. Prodan, and P. Nordlander, Nano Lett. **9**, 887 (2009).
[25] D. C. Marinica, A. K. Kazansky, P. Nordlander, J. Aizpurua, and A. G. Borisov, Nano Lett. **12**, 1333 (2012).
[26] K. J. Savage, M. M. Hawkeye, R. Esteban, A. G. Borisov, J. Aizpurua, and J. J. Baumberg, Nature (London) **491**, 574 (2012).
[27] J. A. Scholl, A. García-Etxarri, A. L. Koh, and J. A. Dionne, Nano Lett. **13**, 564 (2013).
[28] The nonlocality parameter β is given by $\beta = \sqrt{3/5}v_F$. In the present case, the Fermi velocity of conduction electrons $v_F = 1.05 \times 10^6$ m/s resulting in $\beta = 0.81 \times 10^6$ m/s.
[29] Within QCM, the nanowires are described with local Drude permittivity, and the correct tunneling current for the given optical potential is imposed via an "effective" local dielectric constant $\varepsilon_{\text{eff}}(\omega)$ description of the junction. For large junction size $\varepsilon_{\text{eff}}(\omega) \gg 1$, and QCM coincides with the local Drude model.
[30] Because of the small size of the system, the absorption cross section actually calculated with TDDFT can be considered equal to the extinction cross section.
[31] J. H. Parks and S. A. McDonald, Phys. Rev. Lett. **62**, 2301 (1989).
[32] J. Borggreen, P. Chowdhury, N. Kebaïli, L. Lundsberg-Nielsen, K. Lützenkirchen, M. B. Nielsen, J. Pedersen, and H. D. Rasmussen, Phys. Rev. B **48**, 17 507 (1993).
[33] T. Reiners, C. Ellert, M. Schmidt, and H. Haberland, Phys. Rev. Lett. **74**, 1558 (1995).
[34] J. Tiggesbäumker, L. Köller, K.-H. Meiwes-Broer, and A. Liebsch, Phys. Rev. A **48**, R1749 (1993).
[35] L. Serra and A. Rubio, Phys. Rev. Lett. **78**, 1428 (1997).
[36] J. A. Scholl, A. L. Koh, and J. A. Dionne, Nature (London) **483**, 421 (2012).
[37] In the local classical Drude and in the QCM calculations the plasma frequency was set to $\omega_p = 5.74$ eV (close to the nominal value of 5.89 eV). The NLHD needs a larger correction to compensate for the blueshift inherent to this treatment, so here we used $\omega_p = 5.5$ eV.
[38] J. P. Kottmann and O. J. F. Martin, Opt. Express **8**, 655 (2001).
[39] K. Halterman, J. M. Elson, and S. Singh, Phys. Rev. B **72**, 075429 (2005).
[40] I. Romero, J. Aizpurua, G. W. Bryant, and F. J. García de Abajo, Opt. Express **14**, 9988 (2006).
[41] L. Stella, P. Zhang, F. J. García-Vidal, A. Rubio, and P. García-Gonzalez, J. Phys. Chem. C **117**, 8941 (2013).
[42] D. Y. Lei, A. Aubry, Y. Luo, S. A. Maier, and J. B. Pendry, ACS Nano **5**, 597 (2011).
[43] M. Danckwerts and L. Novotny, Phys. Rev. Lett. **98**, 026104 (2007).
[44] J. Lermé, B. Palpant, B. Prével, M. Pellarin, M. Treilleux, J. L. Vialle, A. Perez, and M. Broyer, Phys. Rev. Lett. **80**, 5105 (1998).